PPr701 Project Report
on

Helioseismic Inversion for Rotation Rate

submitted by

Vishal Sai Vetrivel

Roll No: P0211557

Under the guidance of

Prof. H.M Antia



Department of Physical Sciences

Centre for Excellence in Basic Sciences

Mumbai - 400098

December 2024



Certificate

This is to clarify that CEBS student Vishal Sai Vetrivel has undertaken project work from 20th May 2024 to 30th November 2024 under the guidance of Prof. H M Antia
This submitted project report titled Helioseismic Inversion for Rotation Rate is towards the academic requirements of the M.Sc. program's 7th Semester Project Course at UM-DAE CEBS.



Name and Signature of Student with Date



Name and Signature of Advisor(s) with Date

1

Acknowledgments

I would like to express my gratitude to my guide Prof. H M Antia for his invaluable feedback in the writing of this report.

I would also like to thank Dr. Jørgen Christensen-Dalsgaard for publicly uploading his Lecture notes on Stellar Oscillations.

I would also like to thank Red Bull and my roommate for keeping me company through the many sleepless nights.

Abstract

Helioseismology, the study of the solar interior using oscillations obtained from the Solar Surface has been instrumental in our understanding of solar structure and dynamics. The high accuracy with which these observations can be made in the case of the Sun allow for us to make confident inferences on our Solar and Stellar models. We shall go over the various methods that go into the study of solar oscillations. We provide the basic theory of stellar oscillations and outline the approximations involved.

Contents

1 Introduction **5**
- 1.1 Observations of Solar Oscillations . . . 6
  - 1.1.1 Important Instruments . . . 6

2 Hydrodynamical Analysis of Solar Oscillations **7**
- 2.1 Basic Equations of Hydrodynamics . . . 7
- 2.2 Equilibrium State and Perturbation Analysis . . . 8
  - 2.2.1 Perturbed equations . . . 8
- 2.3 Simple Waves . . . 9
  - 2.3.1 Acoustic Waves . . . 9
  - 2.3.2 Internal Gravity Waves . . . 9
  - 2.3.3 Surface Gravity Waves . . . 10

3 The Equations of Linear Oscillations **11**
- 3.1 The Oscillation Equations . . . 11
- 3.2 Linear and Adiabatic Oscillations . . . 13
  - 3.2.1 Boundary Conditions . . . 14

4 Properties of Stellar and Solar Oscillations **14**
- 4.1 The Cowling Approximation . . . 14
- 4.2 Trapping of the Modes . . . 15
- 4.3 p Modes . . . 17
- 4.4 g Modes . . . 18
  - 4.4.1 Numerical Results . . . 19
- 4.5 Functional Analysis of Adiabatic Oscillations . . . 19

5 Rotation and Stellar Oscillations **20**
- 5.1 Effects of a large scale velocity on the oscillation frequencies . . . 20
  - 5.1.1 Pure Rotation . . . 21

1. Introduction

Helioseismology is the study of the structure and dynamical properties of the Sun by its oscillations. These oscillations are the normal modes of the Sun. The oscillations can be predicted from theory and matched through observations to verify or correct the Solar model. There are two different ways to study solar oscillations. The first is the observe integrated light over the whole disk and the second is to observe the Doppler shift at a grid of points over time. The first method is only sensitive to oscillations with large wavelength in relation with solar radius whereas the second method method is much more sensitive. Integrated light measurements are useful as they are the only method available to far away stars.

Measurements are usually repeated at intervals of 1 min giving a Nyquist frequency of $1/2\Delta T = 1/120 = 8.333mHz$. This is the upper limit of frequencies that can be observed without aliasing. The resolution is determined from length of measurement as $1/T$. For a whole day of observation the resolution is 11.6μHz and for a whole year it is 31.6 nHz.

The time over which one measures the Sun is of paramount importance in helioseismology.

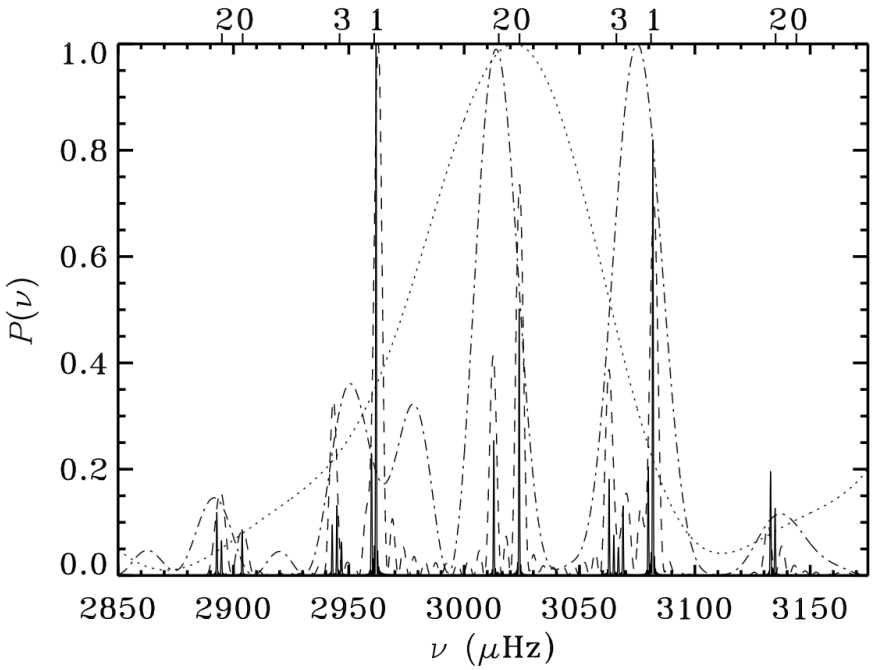


Figure 1.1: Here we see the power spectrum of a simulated time series with random amplitudes and phases for 600 hrs (—), 60 hrs (- - -), 10 hrs (- · - · -) and 3 hrs (· · ·). We can see that for 600 hrs the spectrum is completely resolved, for 60 hrs the rotational splitting is unresolved and for lower times we see that degrees of same parity merge and fictional peaks may appear.[2]

This figure is taken from the Lecture notes on Stellar Oscillations by Christensen-Dalsgaard

It is also important to get uninterrupted measurements as introducing gaps into the time strings can lead to more interference in the final spectrum. Periodic interruptions to measurements lead to a modulation in the spectrum. If more measurements are combined this effect can be minimized to a certain extent however they never go away entirely. Many additional peaks are created with at least two separated from the main peak by $\delta\omega = {}^{2\pi}/_{\tau}$. Here τ is the time when the measurement is resumed. Alternatively $\tau - T$ is the interval between measurements. If the interruptions are random they can be denoted by a window function and calculated on the final spectrum using the fact that the spectrum is a convolution of the window function and the spectrum which allows the final power spectrum to

be a written in terms of the power spectrum of the window function and the original power spectrum. If they window function's transform doesn't overlap too much with the spectrum then the spectrum simply consists of copies of the transformed window function centered around the 'true' frequencies. If they do overlap the situation is much more complicated and results in interference.

Nowadays most instruments either coordinate with multiple locations or position themselves suitably in space to obtain uninterrupted coverage.

While we will mostly be considering adiabatic oscillations this limits our analysis of stability and instability. In adiabatic oscillations there is no energy loss or gain which means there is no possibility of damped modes or self-excited modes where the growth rate is positive. Even in cases where the modes are damped they can still be driven to observable amplitudes by stochastic driving from near-surface convection. This is what appears to be the case in Solar Oscillations.

1.1 Observations of Solar Oscillations

Solar oscillations were first observed by Leighton et al.(1962)[6] who measured velocity fields in the solar atmosphere. They found quasi-periodic motion with a time period of about 5 minutes. Ulrich (1970)[8] and Leibacher and Stein (1971)[5] proposed that these oscillations are the normal modes of the Sun. This was confirmed by observations made by Deubner (1975)[3] who studied the variation of frequencies (ω) with wavenumber (k) and confirmed the predicted behaviour of normal modes of solar oscillations. It was soon realized that these oscillations can be used to study the internal structure of the Sun which lead to the development of Helioseismology.

1.1.1 Important Instruments

Many instruments have been used over the last few decades to obtain data for the study of Solar Oscillations. A few of them are:-

1. **BiSON (Birmingham Solar Oscillation Network)**

   The Birmingham Solar-Oscillations Network (BiSON) is operated by the Solar and Stellar Physics Group at the University of Birmingham, UK. This world-wide network of six remotely operated ground-based telescopes provides round-the-clock monitoring of the globally coherent, core-penetrating modes of oscillation of the Sun. BiSON only measures oscillations through integrated light. BiSON is funded by the UK Science and Technology Facilities Council (STFC)[4]. The six stations are located at Mount Wilson (USA), Las Campanas (Chile), Sutherland (South Africa), Izaña (Tenerife), Carnarvon (Western Australia) and Narrabri (New South Wales, Australia).

2. **GONG (Global Oscillations Network Group)**

   GONG is a worldwide network of six identical telescopes designed to obtain 24/7 measurements of the Sun. They were installed in 1995 at six locations, Big Bear Solar Observatory (South California), Learmouth Solar Observatory (Australia), Udaipur Solar Observatory (India), El Teide Observatory (Canary Islands), Cerro Tololo Interamerican Observatory (Chile) and the Mauna Loa Observatory (Hawaii) respectively. The GONG instrumentation is designed to measure velocity measurements on the surface of the Sun using the photospheric Ni 6768Å line. It gives a time series of 108 days. The observations were staggered by 36 days and it could provide frequencies of Solar oscillations with $l < 150$.

3. **MDI (Michelson Doppler Imager)**

   The MDI is capable of measure spectral intensity and velocities over the full disk or a high resolution field[7]. It provided frequencies on oscillations with degree $l < 300$ It was the biggest contributor to SOHO's data collection with two of the virtual channels being named for it. The MDI has not been used for scientific observation since 2011 as it has been superseded by the Solar Dynamics Observatory's Helioseismic and Magnetic Imager. MDI data sets span a period

of 72 days.[1] The MDI had a 1024x1024 CCD to observe the Sun however only 256x256 was used for continuous data. It is part of SOHO which was launched in 1995. It was turned off in 2011 as its successor HMI was launched and operational.

4. **HMI (Helioseismic and Magnetic Imager)**

   The HMI, led from Stanford University, takes high resolution images of the whole Sun disk with a range focused on the solar spectrum's Fraunhofer line (627.3 nm). It is an updated version of the MDI. It is capable of generating Doppler images and Magnetograms. It is housed in the SDO which was launched in 2010 and is still functional. Like the MDI it has the same 72 day time series and measures up to $l < 300$.

2. Hydrodynamical Analysis of Solar Oscillations

2.1 Basic Equations of Hydrodynamics

We have to deal with two different descriptions of quantities. The **Eulerian** description gives the value of a quantity at a position and time i.e. $p(\boldsymbol{r}, t)$. Whereas the **Lagrangian** description follows the motion of gas. We label functions of the properties using time and the initial position $\boldsymbol{r_0}$ which is the position of the fluid element at time t_0 i.e. $p(\boldsymbol{r_0}, t)$

The time derivative when following the motion is given by:-

$$\frac{d\phi}{dt} = \left(\frac{\partial \phi}{\partial t}\right)_{\boldsymbol{r}} + \left(\frac{\partial \boldsymbol{r}}{\partial t} \cdot \nabla\right) \phi = \left(\frac{\partial \phi}{\partial t}\right)_{\boldsymbol{r}} + (\boldsymbol{v} \cdot \nabla)\, \phi \tag{2.1}$$

Here Φ is some quantity, $\boldsymbol{v}$ is the velocity of the fluid element and the time derivative d/dt following the motion is called the material time derivative whereas $\partial/\partial t$ is known as the local time derivative. Some other basic equations are the equation of continuity:-

$$\frac{\partial \rho}{\partial t} + \operatorname{div}(\rho \boldsymbol{v}) = 0 \tag{2.2}$$

Here ρ is the density and $\boldsymbol{v}$ is the velocity of the fluid element.

Under Stellar conditions we can usually ignore viscosity. This gives us the equation of motion:-

$$\rho \frac{\partial \boldsymbol{v}}{\partial t} + \rho \boldsymbol{v} \cdot \nabla \boldsymbol{v} = -\nabla p - \rho \nabla \Phi \tag{2.3}$$

where p is pressure of the fluid element and Φ is gravitational potential and it satisfies Poisson's equation

$$\nabla^2 \Phi = 4\pi G \rho \tag{2.4}$$

or the integral form

$$\Phi(\boldsymbol{r}, t) = -G \int_V \frac{\rho(\boldsymbol{r}', t)\, \mathrm{d}V}{|\boldsymbol{r} - \boldsymbol{r}'|} \tag{2.5}$$

We will mostly be using the adiabatic approximation in our analysis of solar oscillations. This gives the relation:-

$$\frac{dp}{dt} = \frac{\Gamma_1 p}{\rho} \frac{d\rho}{dt} \tag{2.6}$$

This approximation is valid as the time scales for heat exchange is usually much larger than the oscillation time periods which are around five minutes in the solar case. This is however not true near the surface. Since the sound speed is low near the surface the frequency is affected by it however this contribution can be filtered out through inversions and other analysis.

2.2 Equilibrium State and Perturbation Analysis

A complete general solution of solar oscillations using the equations shown would be far too complex to solve analytically and numerically. Fortunately, in the case of solar oscillations the observed oscillations have small amplitudes compared to the characteristic scales of the Sun. Hence, we may treat the oscillations as a small perturbation about a static equilibrium state. This allows us to linearise the otherwise non-linear equations.

The equilibrium structure is assumed to be static (i.e. all time derivatives vanish) and spherically symmetric. We shall write equilibrium quantities with a subscript 0 and we add a $'$ to denote the perturbations. We also assume there are no velocities in the equilibrium state for the time being. Equation (2.2) is trivially satisfied and the equation of motion (2.3) reduces to the equation of hydrostatic support:-

$$\nabla p_0 = \rho_0 \boldsymbol{g}_0 \tag{2.7}$$

where p_0 is the pressure, ρ_0 is the density and $\boldsymbol{g}_0$ is the gravitational acceleration at equilibrium.

2.2.1 Perturbed equations

We consider small oscillations about the equilibrium state. The perturbed quantities are given as follows:-

$$p(\boldsymbol{r}, t) = p_0(\boldsymbol{r}, t) + p'(\boldsymbol{r}, t) \tag{2.8}$$

Here p' is the Eulerian perturbation. The Lagrangian perturbation would be:-

$$\delta p = p'(\boldsymbol{r}_0) + \boldsymbol{\delta r} \cdot \nabla p_0 \tag{2.9}$$

The equation of continuity becomes:-

$$\frac{\partial \rho'}{\partial t} + \text{ div } (\rho_0 \boldsymbol{v}) = 0 \tag{2.10}$$

here $\boldsymbol{v} = \frac{d\boldsymbol{\delta r}}{dt}$ which allows the continuity equation to be integrated giving:-

$$\rho' + \text{ div } (\rho_0 \boldsymbol{\delta r}) = 0 \tag{2.11}$$

here ρ is density and $\boldsymbol{\delta r}$ is the Lagrangian displacement.

The equation of motion becomes:-

$$\begin{aligned} \rho_0 \frac{\partial^2 \boldsymbol{\delta r}}{\partial t^2} = \rho_0 \frac{\partial \boldsymbol{v}}{\partial t} &= -\nabla p' + \rho_0 \boldsymbol{g}' + \rho' \boldsymbol{g}_0 \\ &= -\nabla p' - \rho_0 \boldsymbol{\nabla \Phi'} + \rho' \boldsymbol{g}_0 \end{aligned} \tag{2.12}$$

The adiabatic energy equation becomes:-

$$\delta p = \frac{\Gamma_{1,0} p_0}{\rho_0} \delta \rho \tag{2.13}$$

In the Eulerian form this can be written as:-

$$\begin{aligned} p' + \boldsymbol{\delta r} \cdot \nabla p_0 &= \frac{\Gamma_{1,0} p_0}{\rho_0} \left(\rho' + \boldsymbol{\delta r} \cdot \nabla \rho_0 \right) \\ &= c_0^2 \left(\rho' + \boldsymbol{\delta r} \cdot \nabla \rho_0 \right) \end{aligned} \tag{2.14}$$

Here c_0^2 is the sound speed given by

$$c_0^2 = \frac{\Gamma_{1,0} p_0}{\rho_0} \tag{2.15}$$

and Γ_1 is the adiabatic exponent defined by

$$\Gamma_1 = \left(\frac{\partial \ln p}{\partial \ln \rho} \right)_{\text{ad}} \tag{2.16}$$

2.3 Simple Waves

2.3.1 Acoustic Waves

We take the simplest possible equilibrium situation and consider the spatially homogeneous case. Here all derivatives of equilibrium quantities vanish. If density is constant then gravity will be zero which can be seen from equation (2.7). Such a situation clearly cannot be realized exactly. However, if the equilibrium structure varies slowly compared with the oscillations, this is a reasonable approximation. We also neglect the perturbation to the gravitational potential as for rapidly varying perturbations regions with positive and negative ρ' nearly cancel. Finally, we assume the adiabatic approximation. If we take divergence of the equation of motion (2.12) with some substitution from the equation of continuity (2.11) we get

$$\frac{\partial^2 \rho'}{\partial t^2} = c_0^2 \nabla^2 \rho' \tag{2.17}$$

where

$$c_0^2 = \frac{\Gamma_{1,0} p_0}{\rho_0} \tag{2.18}$$

Since this is a wave equation we can put in plane wave solutions of the form $\rho' = a \exp\left[i\left(\boldsymbol{k}\cdot\boldsymbol{r} - \omega t\right)\right]$. This gives us the dispersion relation

$$\omega^2 = c_0^2 \left|\boldsymbol{k}\right|^2 \tag{2.19}$$

We see that these are essentially plane sound waves with a sound speed given by c_0^2.

2.3.2 Internal Gravity Waves

We can also take a slightly more complicated case where we consider a layer of gas stratified under gravity. This leads to the presence of a pressure gradient. However, we neglect the gradients of the equilibrium quantities with respect to the perturbations. We also neglect the perturbation to gravitational potential as before. We assume a wave equation solution of the form $(a \exp\left[i\left(\boldsymbol{k}\cdot\boldsymbol{r} - \omega t\right)\right])$ for all the perturbations from the beginning to simplify the analysis. We also separate the displacement $\boldsymbol{\delta r}$ and wave vector $\boldsymbol{k}$ into their radial and horizontal components as follows:-

$$\begin{aligned}\boldsymbol{\delta r} &= \xi_r \hat{\boldsymbol{a}_r} + \boldsymbol{\xi}_h \\ \boldsymbol{k} &= k_r \hat{\boldsymbol{a}_r} + \boldsymbol{k}_h\end{aligned}$$

The radial and horizontal components of the equation of motion (2.12) are:-

$$\begin{aligned}-\rho_0 \omega^2 \xi_r &= -i k_r p' - \rho' g_0 \\ -\rho_0 \omega^2 \boldsymbol{\xi}_h &= -\boldsymbol{k}_h p'\end{aligned}$$

The equation of continuity becomes:-

$$\rho' + \rho_0 i k_r \xi_r + \rho_0 i \boldsymbol{k}_h \cdot \boldsymbol{\xi}_h = 0$$

This gives the pressure perturbation as:-

$$p' = \frac{\omega^2}{k_h^2}\left(\rho' + i k_r \rho_0 \xi_r\right) \tag{2.20}$$

If we assume the frequency is small using these equations we can obtain:-

$$\rho_0 \omega^2 \left(1 + \frac{k_r^2}{k_h^2}\right) \xi_r = \rho' g_0 \tag{2.21}$$

This equation has a simple physical meaning where the buoyancy acting on the density perturbation gives a vertical force that drives the motion. The left hand of the equation gives the vertical acceleration times the mass per unit volume, however, this is modified by the wave numbers which arises from the

pressure perturbation as in order to move vertically a blob of gas must be displaced horizontally, which increases its effective inertia. This effect is stronger when the horizontal wavelength of the perturbation is large.

The adiabatic relation (2.14) gives:-

$$\rho' = c_0^{-2} p' + \rho_0 \boldsymbol{\delta r} \cdot \left(\frac{1}{p_0 \Gamma_{1,0}} \nabla p_0 - \frac{1}{\rho_0} \nabla \rho_0 \right) \tag{2.22}$$

However in this relation the first term can be neglected. We need to eliminate the acoustic modes so we assume the fluid is incompressible except in the $\rho' g_0$ term. This implies $c_0^2 \to \infty$ which means the first term can be dropped.

Combining the left over terms with equation (2.21) we finally get:-

$$\omega^2 \left(1 + \frac{k_r^2}{k_h^2} \right) \xi_r = N^2 \xi_r \tag{2.23}$$

where N^2 is the Brunt–Väisälä frequency given by:-

$$N^2 = g_0 \left(\frac{1}{\Gamma_{1,0}} \frac{d \ln p_0}{dr} - \frac{d \ln \rho_0}{dr} \right) \tag{2.24}$$

From these equations we can obtain the dispersion relation:-

$$\omega^2 = \frac{N^2}{1 + k_r^2 / h_h^2} \tag{2.25}$$

This corresponds to oscillatory motion when $N^2 > 0$. We also note that when the horizontal wavelength is very small the oscillation frequency tends to N. If the horizontal wavelength is not too small then the oscillatory frequency is reduced. These waves are called internal gravity waves which are not to be confused with gravitational waves from general relativity.

The oscillatory condition ($N^2 > 0$) can also be written as

$$\frac{d \ln \rho_0}{d \ln p_0} > \frac{1}{\Gamma_{1,0}} \tag{2.26}$$

When this isn't true the oscillation frequency becomes imaginary and the perturbation grows exponentially with time till it breaks down into turbulence due to non linear effects. Which means that these waves cannot propagate inside the convective layer. This condition is known as the Ledoux Condition (2.26).

$$\frac{d \ln T_0}{d \ln p_0} < \left(\nabla_{\text{ad}} = \frac{\Gamma_{2,0} - 1}{\Gamma_{2,0}} \right) \tag{2.27}$$

Another condition which is the same if the chemical composition is homogeneous is the Schwarzschild criterion (2.27). This condition isn't the same as the Ledoux Condition in general as inside the convection zone the material is mixed and there is no composition gradient. However, it is used in calculations as it is computationally convenient.

2.3.3 Surface Gravity Waves

Apart from the gravity waves described above there is a distinct type of gravity waves similar to waves seen on earth on our oceans. The difference is that these waves occur at a discontinuity in density.

We consider a liquid with constant density ρ_0 with a free surface. This implies the pressure at the surface is constant. The layer is infinitely deep and we assume that the liquid is incompressible. This implies that ρ_0 is constant and $\rho' = 0$. From the equation of continuity we get:-

$$\operatorname{div} \boldsymbol{v} = 0 \tag{2.28}$$

From the equation of motion we get:-

$$\nabla^2 p' = 0 \tag{2.29}$$

We assume a solution of the form $p'(x,z,t) = f(z)\cos(k_h x - \omega t)$ where x is a horizontal coordinate along the surface, z is a vertical coordinate that increases downwards with $z = 0$ at the free surface. This gives us the equation

$$\frac{d^2 f}{dz^2} = k_h^2 f \tag{2.30}$$

Which gives exponential solutions of the form

$$f(z) = a\exp(-k_h z) + b\exp(k_h z) \tag{2.31}$$

Since the layer is infinitely deep $b = 0$. We take the boundary condition at the free surface since the pressure is constant the Lagrangian pressure perturbation vanishes.

$$0 = \delta p = p' + \boldsymbol{\delta r}\cdot\nabla p_0 = p' + \xi_z \rho_0 g_0 \tag{2.32}$$

[1]

This gives

$$\xi_z = -\frac{k_h}{\rho_0\omega^2}p' \tag{2.33}$$

Combining the above equations we get the dispersion relation

$$\omega^2 = g_0 k_h \tag{2.34}$$

We see that the frequencies of these waves do not depend on the internal structure of the layer but only on their wavelength and gravity.

3. The Equations of Linear Oscillations

We now generalize our perturbations to account for non radial oscillations. Radial oscillations or spherically symmetric oscillations are simply a special case of these oscillations. We can separate the time dependence of the perturbations as $\exp(-i\omega t)$. This is possible as the equations do not depend on time.

3.1 The Oscillation Equations

From now on we shall separate the displacement into its radial and horizontal components as follows.

$$\boldsymbol{\delta r} = \xi_r \hat{\boldsymbol{a}_r} + \boldsymbol{\xi}_h \tag{3.1}$$

The equation of continuity (2.11) can be written as follows:-

$$\rho' = -\frac{1}{r^2}\frac{\partial}{\partial r}\left(\rho_0 r^2 \xi_r\right) - \rho_0 \nabla_h \cdot \boldsymbol{\xi}_h \tag{3.2}$$

The radial component of the linearized equation of motion (2.12) is:-

$$\rho\frac{\partial^2 \xi_r}{\partial t^2} = -\frac{\partial p'}{\partial r} - \rho' g_0 - \rho_0\frac{\partial \Phi'}{\partial r} \tag{3.3}$$

The horizontal component yields the following:-

$$-\frac{\partial^2}{\partial t^2}\left[\rho' + \frac{1}{r^2}\frac{\partial}{\partial r}\left(r^2\rho_0\xi_r\right)\right] = -\nabla_h^2 p' - \rho_0\nabla_h^2\Phi' \tag{3.4}$$

Poisson's equation can also be written as:-

$$\frac{1}{r^2}\frac{\partial}{\partial r}\left(r^2\frac{\partial \Phi'}{\partial r}\right) + \nabla_h^2\Phi' = 4\pi G\rho' \tag{3.5}$$

[1] Derivation is in appendix

We note that all the derivatives of θ and ϕ only appear in combination with ∇_h^2. We would now like to separate the angular dependence of perturbations as a function $f(\theta, \phi)$. If we write out the full form of ∇_h^2 and work out an eigenvalue problem we will see that $f(\theta, \phi)$ are Spherical Harmonics.

$$f(\theta, \phi) = Y_l^m(\theta, \phi) = (-1)^m c_{lm} P_l^m (\cos\theta) \exp(im\phi) \tag{3.6}$$

Here c_{lm} is a normalization constant such that $\int\limits_{\text{unit sphere}} |Y_l^m|^2 \, d\Omega = 1$. Another property of Y_l^m is that it satisfies.

$$\nabla_h^2 Y_l^m = -\frac{l(l+1)}{r^2} Y_l^m \tag{3.7}$$

Now we write the variables in equations (3.3) and (3.4) can be written in terms of spherical harmonics as plane waves are not applicable for spherical coordinates.

Scalar quantities such as p' are given as follows:-

$$p'(r, \theta, \phi, t) = \sqrt{4\pi}\tilde{p}'(r) Y_l^m(\theta, \phi) \exp(-i\omega t) \tag{3.8}$$

The displacement can be written as follows:-

$$\boldsymbol{\delta r} = \sqrt{4\pi} Re \left\{ \left[\tilde{\xi_r}(r) Y_l^m(\theta, \phi) \boldsymbol{a}_r + \tilde{\xi_h}(r) \left(\frac{\partial Y_l^m}{\partial \theta} \boldsymbol{a}_\theta + \frac{1}{\sin\theta} \frac{\partial Y_l^m}{\partial \phi} \boldsymbol{a}_\phi \right) \right] \exp(-i\omega t) \right\} \tag{3.9}$$

where

$$\tilde{\xi_h}(r) = \frac{1}{r\omega^2} \left(\frac{\tilde{p}'}{\rho_0} + \tilde{\Phi}' \right) \tag{3.10}$$

Putting these into the linearized equations given above we get:-

$$\omega^2 \left[\tilde{\rho}' + \frac{1}{r^2} \frac{d}{dr} \left(r^2 \rho_0 \tilde{\xi_r} \right) \right] = \frac{l(l+1)}{r^2} \left(\tilde{p}' + \rho_0 \tilde{\Phi}' \right) \tag{3.11}$$

$$\omega^2 \rho_0 \tilde{\xi_r} = -\frac{d\tilde{p}'}{dr} - \tilde{\rho}' g_0 - \rho_0 \frac{d\tilde{\Phi}'}{dr} \tag{3.12}$$

$$\frac{1}{r^2} \frac{d}{dr} \left(r^2 \frac{d\tilde{\Phi}'}{dr} \right) - \frac{l(l+1)}{r^2} \tilde{\Phi}' = 4\pi G \tilde{\rho}' \tag{3.13}$$

And the adiabatic relation:-

$$\delta p = \frac{\Gamma_{1,0} p_0}{\rho_0} \delta\rho = c_0^2 \delta\rho \tag{3.14}$$

where c_0^2 is the sound speed given by $c_0^2 = \frac{\Gamma_{1,0} p_0}{\rho_0}$

It should be noted that none of these 4 equations involve the azimuthal order m. This is a consequence of the assumed spherical symmetry of the equilibrium state.

The frequency is real for adiabatic oscillations. We now calculate the mean squared components of displacement.

$$\delta r_{rms}^2 = \frac{1}{2} \left| \tilde{\xi_r}(r) \right|^2 \tag{3.15}$$

Similarly the horizontal component of $\boldsymbol{\delta r}$ is

$$\delta h_{rms}^2 = \frac{l(l+1)}{2} \left| \tilde{\xi_h}(r) \right|^2 \tag{3.16}$$

The kinetic energy of pulsation is

$$E_{kin} = \frac{1}{2} \int_V |\boldsymbol{v}|^2 \rho_0 \mathrm{d}V \tag{3.17}$$

The time averaged energy is $1/4\omega^2\mathcal{E}$ where

$$\mathcal{E} = 4\pi \int_0^R \left[\left| \tilde{\xi}_r(r) \right|^2 + l(l+1) \left| \tilde{\xi}_h(r) \right|^2 \right] \rho_0 r^2 \mathrm{d}r \tag{3.18}$$

It is convenient to introduce the dimensionless measure E of $\mathcal{E}$ by:-

$$E = \frac{4\pi \int_0^R \left[\left| \tilde{\xi}_r(r) \right|^2 + l(l+1) \left| \tilde{\xi}_h(r) \right|^2 \right] \rho_0 r^2 \mathrm{d}r}{M \left[\left| \tilde{\xi}_r(R) \right|^2 + l(l+1) \left| \tilde{\xi}_h(R) \right|^2 \right]} = \frac{M_{\mathrm{mode}}}{M} \tag{3.19}$$

where M is the total mass of the Sun and M_{mode} is the modal mass of the Sun. E provides a measure of the normalized inertia of the mode. This normalization is useful as eigenfunctions are arbitrary to a constant multiple so we divide them by a similar combination. This definition also gives the following expression for the time averaged kinetic energy:-

$$\frac{1}{2} M_{\mathrm{mode}} V_r^2 ms = \frac{1}{2} E M V_{rms}^2 \tag{3.20}$$

3.2 Linear and Adiabatic Oscillations

Note, we drop the $_0$ subscript for the equilibrium quantities and the tilde on amplitude functions. For adiabatic oscillations we get a relation for ρ' from equation (2.22):-

$$\rho' = c_0^{-2} p' + \rho_0 \boldsymbol{\delta r} \cdot \left(\frac{1}{p_0 \Gamma_{1,0}} \nabla p_0 - \frac{1}{\rho_0} \nabla \rho_0 \right)$$

This can be used to eliminate ρ' from the earlier equations, yielding:-

From (3.11)

$$\frac{d\xi_r}{dr} = -\left(\frac{2}{r} + \frac{1}{\Gamma_1 p} \frac{dp}{dr} \right) \xi_r + \frac{1}{\rho c^2} \left(\frac{S_l^2}{\omega^2} - 1 \right) p' + \frac{l(l+1)}{\omega^2 r^2} \Phi' \tag{3.21}$$

From (3.12)

$$\frac{dp'}{dr} = \rho \left(\omega^2 - N^2 \right) \xi_r + \frac{1}{\Gamma_1 p} \frac{dp}{dr} p' - \rho \frac{d\Phi'}{dr} \tag{3.22}$$

From (3.13)

$$\frac{1}{r^2} \frac{d}{dr} \left(r^2 \frac{d\Phi'}{dr} \right) = 4\pi G \left(\frac{p'}{c^2} + \frac{\rho \xi_r}{g} N^2 \right) + \frac{l(l+1)}{r^2} \Phi' \tag{3.23}$$

Here S_l is the characteristic acoustic frequency and is given by:-

$$S_l^2 = \frac{l(l+1) c^2}{r^2} = k_h^2 c^2 \tag{3.24}$$

These three equations constitute a fourth order system of ordinary differential equations for four dependent variables ξ_r, p', Φ' and $\frac{d\Phi'}{dr}$. Thus it is a complete set of differential equations.

It should also be noticed that all the coefficients in these three equations are real, we also see that the boundary conditions are also real. Since frequency only appears as ω^2 we may expect that solution will be such that ω^2 is real, in which case the eigenfunctions can be chosen to be real as well. Thus the frequency ω is either purely real or purely imaginary. In the former case the system is like an undamped oscillatory whereas in the latter case the motion grows or decays exponentially. Physically this arises from the adiabatic condition which states the only energy fed into the motion is from the gravitational field which allows only a dynamical instability.

3.2.1 Boundary Conditions

We need four boundary conditions to supplement the four equations we have in the general case. We provide them by looking at behaviour at the special regions of the equations i.e. the centre and surface.

$r \to 0$	$r = R$
$\xi_r \sim r^{l-1}$	$\frac{d\Phi'}{dr} + \frac{l+1}{r}\Phi' = 0$
$p', \Phi' \sim r^l$	$\delta p = 0$

We can also show that near $r \to 0$ and $l > 0$ we have $\xi_r \simeq l\xi_h$. The $r \to 0$ conditions are set to ensure we get regular solutions from the singular point at $r = 0$. The $\delta p = 0$ is important as we have set the Lagrangian perturbation to zero instead of the Eulerian derivative. This is the same as saying there are no forces on the surface and that the pressure is constant, however the reason it is Lagrangian and not Eulerian is that the perturbations make it so that the surface is not an exact sphere. We require the perturbation to pressure on the surface to be zero hence we set the material derivative to zero.

From this equation we can estimate the ratio between the radial and horizontal components of the displacement on the surface. We can get the amplitude of the horizontal displacement from equation (3.10). We also take the perturbation to gravitational potential to be small. This gives us the approximate relation of:-

$$\frac{\xi_h(R)}{\xi_r(R)} = \frac{g_s}{R\omega^2} = \sigma^{-2} \tag{3.25}$$

where g_s is the surface gravity and σ is a dimensionless frequency given by

$$\sigma^2 = \frac{R^3\omega^2}{GM} \tag{3.26}$$

Thus this ratio only depends on frequency. The ratio of the rms values of the horizontal and vertical can be written using equations (3.16) and (3.15).

$$\frac{\delta h_{\text{rms}}}{\delta r_{\text{rms}}} = \frac{\sqrt{l(l+1)}}{\sigma^2}, \qquad \text{at } r = R \tag{3.27}$$

For the case of the solar five-minute oscillations, $\sigma^2 \sim 1000$ which implies the motion is predominantly radial except when l is large.

4. Properties of Stellar and Solar Oscillations

4.1 The Cowling Approximation

The general equations of oscillations are fourth order which leads to difficulties in analysis. However, fortunately the perturbation to gravitational potential Φ' can often be neglected. To see how we write the integral solution to Poisson's equation:-

$$\Phi'(r) = -\frac{4\pi G}{2l+1}\left[\frac{1}{r^{l+1}}\int_0^r \rho'(r')\, r'^{l+2}\mathrm{d}r' + r^l \int_r^R \frac{\rho'(r')}{r'^{l-1}}\mathrm{d}r'\right] \tag{4.1}$$

We can see that $|\Phi'|$ is small compared with ρ' if:-

i) When l is large

In this case $(r'/r)^{l+2}$ in the first integral is small when $r' < r$ and $(r/r')^{l-1}$ from the second integral is small when $r' > r$. The whole expression is also reduced by a factor

of $(2l+1)$. In essence for large ls the oscillations are trapped near the surface where the density is too low for them to contribute to Φ'. This is discussed in the next section.

ii) When radial order $|n|$ is large

In this case the integrals are over rapidly varying functions of r and is therefore reduced relative to the size of the integrand.

While this reasoning works well for high order or high degree oscillations its full mathematical justification has not yet been analyzed. This is however only used to understand mode classification as all actual calculations are done numerically without any such approximations and the full equations.

4.2 Trapping of the Modes

The equations in the Cowling approximation can be written as

$$\frac{d\xi_r}{dr} = -\left(\frac{2}{r} - \frac{1}{\Gamma_1}H_p^{-1}\right)\xi_r + \frac{1}{\rho c^2}\left(\frac{S_l^2}{\omega^2} - 1\right)p' \tag{4.2}$$

$$\frac{dp'}{dr} = \rho\left(\omega^2 - N^2\right)\xi_r - \frac{1}{\Gamma_1}H_p^{-1}p' \tag{4.3}$$

where H_p is the pressure scale height, i.e. the distance over which the pressure changes by a factor of e. It is given by

$$H_p^{-1} = -\frac{d\ln p}{dr} \tag{4.4}$$

As a first rough approximation we neglect the eigenfunctions with respect to their derivatives. We do this as we assume the scale height of the eigenfunctions are smaller than H_p and r respectively. This also allows us to combine the two equations later. This reduces the equations to:-

$$\frac{d\xi_r}{dr} = \frac{1}{\rho c^2}\left(\frac{S_l^2}{\omega^2} - 1\right)p' \tag{4.5}$$

$$\frac{dp'}{dr} = \rho\left(\omega^2 - N^2\right)\xi_r \tag{4.6}$$

These two equations can be combined into a single second order differential equation for ξ_r:-

$$\frac{d^2\xi_r}{dr^2} = \frac{\omega^2}{c^2}\left(1 - \frac{N^2}{\omega^2}\right)\left(\frac{S_l^2}{\omega^2} - 1\right)\xi_r \tag{4.7}$$

This equation holds many questionable approximations as the terms that are neglected aren't always small, such as $2/r$ which is large near the core. However the equation is adequate to describe the overall properties of the modes of oscillation.

If we write the previous equation in the form

$$\frac{d^2\xi_r}{dr^2} = -K(r)\,\xi_r \tag{4.8}$$

where

$$K(r) = \frac{\omega^2}{c^2}\left(\frac{N^2}{\omega^2} - 1\right)\left(\frac{S_l^2}{\omega^2} - 1\right) \tag{4.9}$$

The local behaviour of ξ_r depends on the sign of K. If K is positive then ξ_r is locally an oscillatory function in r, whereas if K is negative then the solution will be exponentially increasing or decreasing in r.

According to this description the solution oscillates when

$$\text{o1)} \qquad |\omega| > |N| \qquad \text{and} \qquad |\omega| > S_l \tag{4.10}$$

or

$$\text{o2)} \qquad |\omega| < |N| \qquad \text{and} \qquad |\omega| < S_l \tag{4.11}$$

and it is exponential when

$$\text{e1)} \qquad |N| < |\omega| < S_l \tag{4.12}$$

or

$$\text{e2)} \qquad S_l < |\omega| < |N| \tag{4.13}$$

For any given mode of oscillation there may be many regions where the conditions o1 or o2 are satisfied and are hence oscillatory. The regions in between will have exponential solutions. In general one of these oscillating regions is dominant and the solution decays exponentially away from it. The solution is then said to be trapped in this region. The frequency is determined majorly by the structure in this region. The boundaries of this region are when $K(r) = 0$. These points are called turning points. We can also see that when K is higher the solution oscillates faster which means the order generally increases with increasing K.

Since different modes are trapped in different regions we get another effect. Modes with low l penetrate deeper where the density is higher and consequently have a higher mode inertia. Mode inertia can be found from equation (3.19). This makes them less sensitive to the perturbations of the surface which are important as it is believed that excitation of modes is due to turbulent convection of the surface layer. If we scale the frequencies by their corresponding mode inertia then we see that the error in the Standard Solar Model with respect to real world data is of the order of 10^{-3} which gives us confidence in the model.

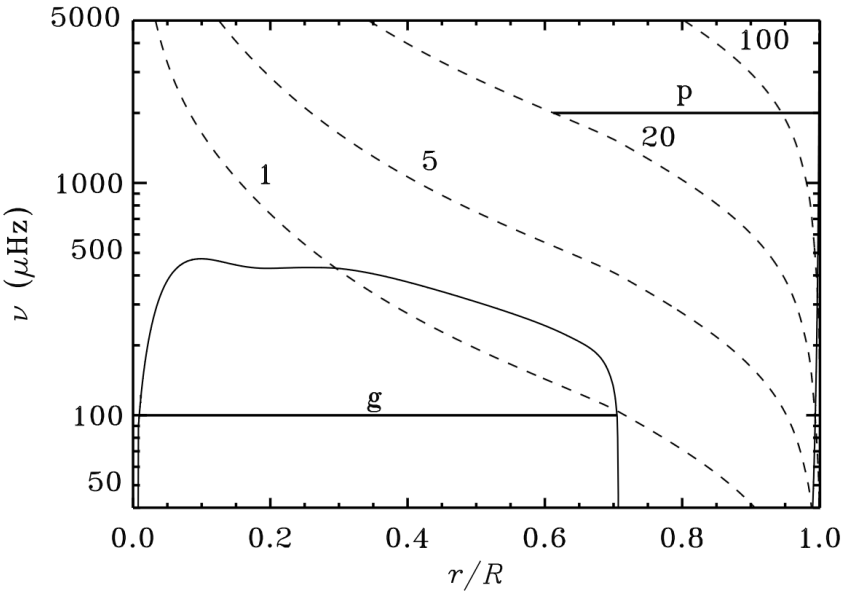


Figure 4.1: Buoyancy frequency N (continuous line) and characteristic acoustic frequency S_l (dashed line) shown in terms of the corresponding cyclic frequencies against fractional radius for a model of the Sun. The heavy horizontal lines show the trapping regions for a g mode with frequency $\nu = 100\,\mu$Hz and for a p mode with degree 20 and $\nu = 2000\,\mu$Hz.
This figure is taken from the Lecture notes on Stellar Oscillations by Christensen-Dalsgaard

In Figure 4.1 the solid line in the bottom left is the buoyancy frequency N as a function of fractional radius. The line is only drawn for real values and we see that it stops somewhere between 0.6 and 0.8 as in the convection zone the value of N is imaginary. The horizontal lines show the trapping regions for typical g and p modes. We see that there is good separation between the two types. This is the

core concept that allows most of the analysis in Helioseismology. We also note that the characteristic acoustic frequency S_l goes to zero near the surface and blows up near the centre of the Sun. This is due to the dependence on sound speed which is higher in regions of high density.

From this figure we see that there are two classes of modes:

i) Modes with high frequencies satisfying o1, labeled p modes

ii) Modes with low frequencies satisfying o2, labeled g modes

4.3 p Modes

P modes are trapped between an inner turning point at $r = r_t$ and the surface. This cannot be done under the approximation we've used as inverse scale height is not negligible near the stellar surface. The inner turning point is located where $S_l(r_t) = \omega$ or

$$\frac{c^2(r_t)}{r_t^2} = \frac{\omega^2}{l(l+1)} \tag{4.14}$$

This determines the turning point as a function of l and ω For p modes especially the five-minute oscillations we have $w \gg N$. This means we can approximate K as

$$K(r) \simeq \frac{1}{c^2}\left(\omega^2 - S_l^2\right) \tag{4.15}$$

This equation can be obtained from the dispersion relation for a plane sound wave. If we identify $K(r) = k_r^2$ then we can see that:-

$$\begin{aligned} |\boldsymbol{k}|^2 &= k_r^2 + k_h^2 \\ |k|^2 &= \frac{\omega^2}{c^2} \\ k_h^2 &= \frac{l(l+1)}{r^2} \\ \implies \frac{\omega^2}{c^2} &= k_r^2 + \frac{l(l+1)}{r^2} \\ \implies k_r^2 &= K(r) = \frac{1}{c^2}\left(\omega^2 - S_l^2\right) \end{aligned}$$

This shows the turning points are the points where $k_r = 0$. Therefore in this approximation the dynamics of p modes only depends on the variation of sound speed with r. These are interpreted as standing acoustic waves with the restoring force being mostly pressure.

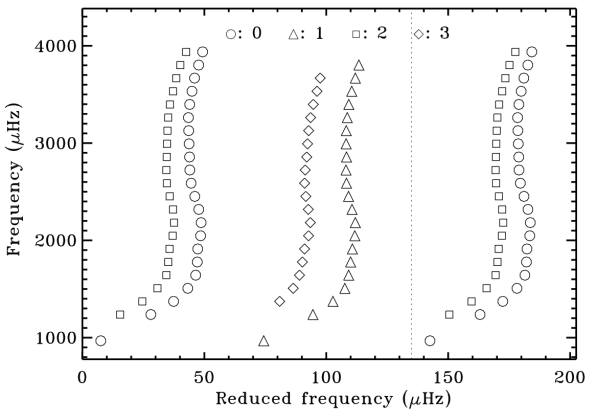


Figure 4.2: Echelle diagram for observed solar frequencies obtained by the BiSON network (Chaplin *etal*. 2002), plotted for $\nu_0 = 830\,\mu$Hz and $\Delta\nu = 135\mu$Hz. The shapes represent the modes of the degree (l).
Note: The points for $l = 0, 2$ are repeated on the right and the dotted line indicates $\Delta\nu$.
Figure taken from Christensen-Dalsgaard's Lecture Notes.

The interior reflection of p modes can be understood in terms of ray theory. A mode can be understood as a superposition of propogating sound waves. As they propagate deeper into the star the sound speed increases, however this causes the direction of propagation to bend away from the radial direction similar to refraction in light. At the reflection point the wave travels horizontally.

Asymptotic analysis of p modes assuming the solar convection zone is approximately adiabatically stratified and Γ_1 and g are constant. We take the boundary conditions $p = \rho = 0$ at $r = R$. With these assumptions we get the dispersion relation

$$\omega^2 = \frac{2}{\mu_p}\frac{g}{R}(n+\alpha)L \tag{4.16}$$

where $L^2 = l\,(l+1)$

This states that ω is proportional to $L^{1/2}$. This is seen to be true for frequencies with high degree as they are almost entirely trapped within the convection zone. This equation can also be written as

$$\omega = \frac{(n + L/2 + \alpha)\,\pi}{\int_0^R \frac{\mathrm{d}r}{c}} \tag{4.17}$$

An alternate form of this equation allows us to easily analyze Echelle diagrams for p modes.

$$\nu_{nl} = \frac{\omega_{nl}}{2\pi} \simeq \left(n + \frac{l}{2} + \frac{1}{4} + \alpha\right)\Delta\nu \tag{4.18}$$

where $\Delta\nu = \left[2\int_0^R \frac{\mathrm{d}r}{c}\right]^{-1}$. This expression predicts an almost degeneracy between modes that have the same value of $n + l/2$. This degeneracy can be lifted if this expression is extended by taking into account the variation of sound speed c in the core and by taking the JWKB analysis of the equations to a higher order. This will give the expression:-

$$\nu_{nl} \simeq \left(n + \frac{l}{2} + \frac{1}{4} + \alpha\right)\Delta\nu - \left(AL^2 - \delta\right)\frac{\Delta\nu^2}{\nu_{nl}} \tag{4.19}$$

where

$$A = \frac{1}{4\pi^2\Delta\nu}\left[\frac{c\,(R)}{R} - \int_0^R \frac{dc}{dr}\frac{\mathrm{d}r}{r}\right] \tag{4.20}$$

This gives us an expression for the small frequency separation between apparently degenerate frequencies as:-

$$\delta\nu_{nl} = \nu_{nl} - \nu_{n-1,l+2} \simeq -\,(4L+6)\,\frac{\Delta\nu}{4\pi^2\nu_{nl}}\int_0^R \frac{dc}{dr}\frac{\mathrm{d}r}{r} \tag{4.21}$$

Echelle diagrams are used to find patterns in frequency like the large and small frequency differences in p modes. We essentially stack the frequencies on top of each other in intervals defined by $\Delta\nu$. If the frequencies are from p modes we shall see straight vertical lines. This can be seen in Figure 4.2.

4.4 g Modes

In g modes the turning point positions are determined by the condition $N = \omega$. From 4.1 we see that one of the turning points is near the centre of the Sun and the other is just below the base of the convective zone. At higher frequencies the upper turning point is deeper in the star whereas for lower frequencies the upper turning point is close to where N is maximum. In our approximation however the turning points are independent of l.

For high-order g modes $\omega \ll S_l^2$ which allows us to approximate K as

$$K\,(r) \simeq \frac{\left(N^2 - \omega^2\right)}{\omega^2}\frac{l\,(l+1)}{r^2} \tag{4.22}$$

If we perform similar analysis like we did for the p modes we shall get a relation which allows us to identify $K(r) = k_r^2$, which implies that the turning points can be found by setting k_r to zero. In this case the dynamics are dominated by the variation of buoyancy frequency N with r. The dominant restoring force is gravity acting on the density perturbation. These modes are trapped gravity waves. We see from the above equation that K increases with decreasing ω. Which means the order of the mode increases with decreasing ω. It should be noted that the frequencies of the g modes cannot exceed a maximum $N_{\max}$ which has been analyzed by Christensen-Dalsgaard (1980).

4.4.1 Numerical Results

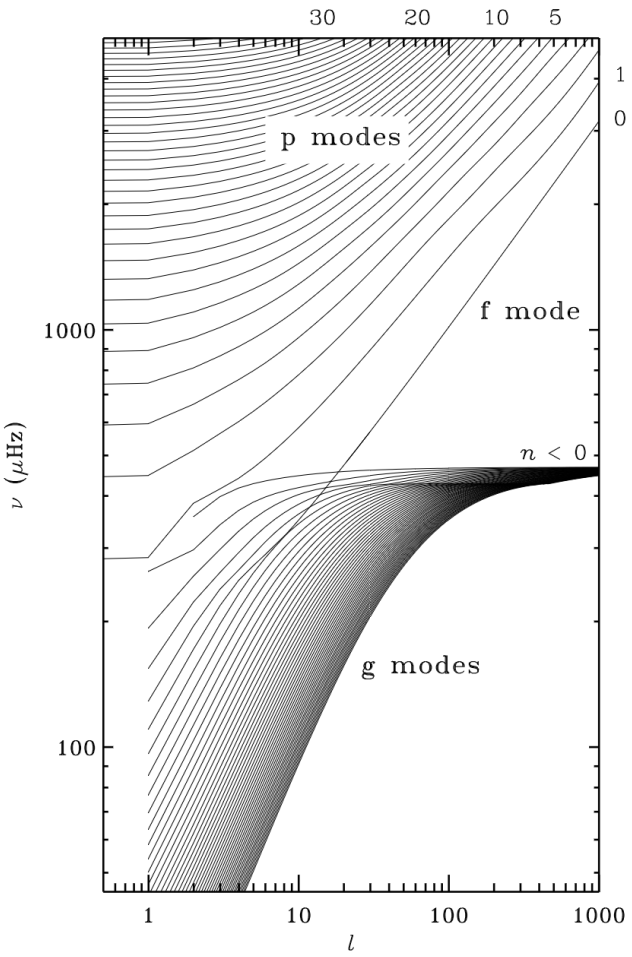


Figure 4.3: Cyclic frequencies $v = \omega/2\pi$ as functions of degree l computed for a normal solar model.
Figure taken from Christensen-Dalsgaard's Lecture Notes.

We can look at numerically simulated results for a normal solar model. In this Figure 4.3 we take l to be a continuously varying value even though only integral values of l have physical meaning. Some of them are also labeled by the radial order which helps give the number of zeros along the radial direction in the eigenfunctions.

The upper set of modes correspond to the p modes described above. We can see that the frequency increases with increase in degree like we expected from the equation above. The modes labeled with 0 behave similarly to p modes but are distinct and are known as f modes. For $l > 20$ their frequencies are given by expression $\omega^2 = g_0 k_h$.

The lower set of modes correspond to g modes. We see that the frequency reduces with the number of nodes. We also see that there is a clear maximum possible frequency. It is also to be noted that in principle all degrees can be extended to $\nu = 0$ however, it would get too crowded. There are also no g modes for $l = 0$ as some variation across horizontal surface is required which doesn't happen in the spherically symmetric $l = 0$ case.

We also note that there are apparent crossings in the two different modes. A closer examination by allowing l to be a continuous variable shows that around the point at which they appear to meet the two lines approach each other but do not actually meet. This phenomenon called avoided crossing and is well understood and known in atomic and quantum physics as it appears in many systems including but not limited to two-level systems.

4.5 Functional Analysis of Adiabatic Oscillations

A large amount of analysis into the properties of adiabatic oscillations can be performed if the we regard the basic equations as an eigenvalue problem in a Hilbert space (Eisenfeld 1969; Dyson and Schutz 1979; Christensen-Dalsgaard 1981). We can write equation (2.12) in the following form:-

$$\omega^2 \boldsymbol{\delta r} = \mathcal{F}(\boldsymbol{\delta r}) \tag{4.23}$$

where

$$\mathcal{F}(\boldsymbol{\delta r}) = \frac{1}{\rho_0}\nabla p' - \boldsymbol{g}' - \frac{\rho'}{\rho_0}\boldsymbol{g}_0 \tag{4.24}$$

This can be done as using the continuity equation, adiabatic equation and certain other equations we can always write our oscillation equations as a eigenvalue problem in $\boldsymbol{\delta r}$.

We introduce a space $\mathcal{H}$ of vector functions which $\boldsymbol{\delta r}$ can be. We also define an inner product on this space

$$\langle \boldsymbol{a}, \boldsymbol{b} \rangle = \int_V \rho_0 \boldsymbol{a}^* \cdot \boldsymbol{b} \mathrm{d}V \tag{4.25}$$

If we only consider the functions which satisfy the boundary conditions then this inner product is symmetric. This leads to many desirable properties, one of which is that squared eigen frequencies are real. Another useful property is orthogonality when two eigenfunctions have different eigenvalues.

Here $\mathcal{F}$ is an operator which defines the model being used in the calculations. Its form was given by Chandrasekhar (1964) who also proved that the operator including some simple boundary conditions was Hermitian. This allows us to perform variational analysis on these operators. Which yields equations of the form:-

$$\frac{\delta\omega_{nl}}{\omega_{nl}} = \frac{\langle \xi_{nl}, \delta\mathcal{F}\left(\xi_{nl}\right)\rangle_l}{2\omega_{nl}\left\langle \xi_{nl}, \xi_{nl}\right\rangle_l} \tag{4.26}$$

where $\delta\mathcal{F}$ is a perturbation to the operator which can arise from change in structure of the Solar model or in our case the addition of rotation in the equations.

5. Rotation and Stellar Oscillations

So far we have assumed that there are no velocity fields in the equilibrium state of our model. This is however an oversimplification as most stars at least rotate. Hence we wish to take these into account.

5.1 Effects of a large scale velocity on the oscillation frequencies

We take an equilibrium structure that is stationary ($\frac{\partial}{\partial t} = 0$). We assume that the equilibrium state is one where there is a non-zero velocity field $\boldsymbol{v_0}$ which is small enough that $|\boldsymbol{v_0}|^2$ can be neglected in our equations.

From (2.2) and because the assumed stationarity we get

$$\text{div}\ (\rho_0 \boldsymbol{v_0}) = 0 \tag{5.1}$$

Using the equation of motion (2.3) and neglecting quadratic terms of $\boldsymbol{v}$ we get:

$$0 = -\nabla p_0 + \rho_0 \boldsymbol{g}_0 \tag{5.2}$$

This shows that the equation of hydrostatic support (2.7) is unchanged under an equilibrium velocity field.

We consider perturbations of the form:-

$$\boldsymbol{v} = \boldsymbol{v}_0 + \boldsymbol{v}' \tag{5.3}$$

The displacement $\boldsymbol{\delta r}$ is related to $\boldsymbol{\delta v}$ as follows:-

$$\frac{d\boldsymbol{\delta r}}{dt} = \boldsymbol{\delta v} = \boldsymbol{v}' + \left(\boldsymbol{\delta r}\cdot\nabla\right)\boldsymbol{v}_0 \tag{5.4}$$

$$\frac{d\boldsymbol{\delta r}}{dt} = \frac{\partial \boldsymbol{\delta r}}{\partial t} + \left(\boldsymbol{v}_0\cdot\nabla\right)\boldsymbol{\delta r} \tag{5.5}$$

The perturbed continuity equation can be written as:-

$$\frac{\partial A}{\partial t} + \text{div}\ (A\boldsymbol{v}_0) = 0 \tag{5.6}$$

where

$$A = \rho' + \text{div}\ (\rho_0 \boldsymbol{\delta r})$$

For this case we obtain the equation of motion as

$$\rho_0 \frac{\partial^2 \boldsymbol{\delta r}}{\partial t^2} + 2\rho_0\left(\boldsymbol{v}_0\cdot\nabla\right)\left(\frac{\partial \boldsymbol{\delta r}}{\partial t}\right) = -\nabla p' + \rho_0 \boldsymbol{g}' + \rho' \boldsymbol{g}_0 \tag{5.7}$$

We notice that the only difference between our original equations and this case is the inclusion of the second term on the LHS i.e. $2\rho_0 (\boldsymbol{v}_0 \cdot \nabla) \left(\frac{\partial \boldsymbol{\delta r}}{\partial t}\right)$. If we assume the form of $\exp(-i\omega t)$ for the time dependence we can get a equation of the form:-

$$-\omega^2 \rho \boldsymbol{\delta r} - 2i\omega\rho_0 (\boldsymbol{v}_0 \cdot \nabla) \boldsymbol{\delta r} = -\nabla p' + \rho_0 \boldsymbol{g}' + \rho' \boldsymbol{g}_0 \tag{5.8}$$

This can be directly compared with the equation used in the functional analysis of oscillations which gives us

$$\delta\mathcal{F} = -2i\omega (\boldsymbol{v}_0 \cdot \nabla) \boldsymbol{\delta r} \tag{5.9}$$

We can now get the change in ω due to the inclusion of velocity field to the first order as:-

$$\delta\omega = -i \frac{\int_V \rho_0 \boldsymbol{\delta r}^* \cdot (\boldsymbol{v}_0 \cdot \nabla) \boldsymbol{\delta r} \, \mathrm{d}V}{\int_V \rho_0 |\boldsymbol{\delta r}|^2 \, \mathrm{d}V} \tag{5.10}$$

5.1.1 Pure Rotation

We can consider the case of pure rotation. In this case the velocity $\boldsymbol{v}_0$ will be given by

$$\boldsymbol{v}_0 = \Omega r \sin\theta \boldsymbol{a}_\phi = \boldsymbol{\Omega} \times \boldsymbol{r} \tag{5.11}$$

Here the rotation is about the axis of the spherical coordinate system. $\Omega = \Omega(r, \theta)$ is a function of θ and r and $\boldsymbol{\Omega} = \Omega(\cos\theta \boldsymbol{a}_r - \sin\theta \boldsymbol{a}_\theta)$ If we repeat the steps from the previous case but with our specific form for $\boldsymbol{v}_0$ we will get the equation of motion as:-

$$-\omega^2 \rho \boldsymbol{\delta r} + 2m\omega\Omega\rho_0 \boldsymbol{\delta r} - 2i\omega\rho_0 \boldsymbol{\Omega} \times \boldsymbol{\delta r} = -\nabla p' + \rho_0 \boldsymbol{g}' + \rho' \boldsymbol{g}_0 \tag{5.12}$$

From this we have our value for $\delta\mathcal{F}$ as:-

$$\delta\mathcal{F} = 2m\omega\Omega \boldsymbol{\delta r} - 2i\omega \boldsymbol{\Omega} \times \boldsymbol{\delta r} \tag{5.13}$$

This can be used with equation (5.10) to find the change in frequency.

Bibliography

[1] H. M. Antia. Helioseismology. In Abhishek Kumar Srivastava, Marcel Goossens, and Inigo Arregui, editors, *Magnetohydrodynamic Processes in Solar Plasmas*, pages 31–74. 2024.

[2] Jørgen Christensen-Dalsgaard. Lectures on stellar oscillations.

[3] F. L. Deubner. Observations of low wavenumber nonradial eigenmodes of the sun. *Astronomy and Astrophysics*, 44(2):371–375, November 1975.

[4] Y. Elsworth, R. Howe, G. R. Isaak, C. P. McLeod, B. A. Miller, H. B. van der Raay, S. J. Wheeler, and R. New. Performance of the BISON Network 1981-Present. In R. K. Ulrich, Jr. Rhodes, E. J., and W. Dappen, editors, *GONG 1994. Helio- and Astro-Seismology from the Earth and Space*, volume 76 of *Astronomical Society of the Pacific Conference Series*, page 392, January 1995.

[5] J. W. Leibacher and R. F. Stein. A New Description of the Solar Five-Minute Oscillation. *Astrophysics Letters*, 7:191–192, January 1971.

[6] Robert B. Leighton, Robert W. Noyes, and George W. Simon. Velocity fields in the solar atmosphere. i. preliminary report. *Astrophysical Journal*, 135:474, March 1962.

[7] P. H. Scherrer, R. S. Bogart, R. I. Bush, J. T. Hoeksema, A. G. Kosovichev, J. Schou, W. Rosenberg, L. Springer, T. D. Tarbell, A. Title, C. J. Wolfson, I. Zayer, and MDI Engineering Team. The Solar Oscillations Investigation - Michelson Doppler Imager. *Solar Physics*, 162(1-2):129–188, December 1995.

[8] Roger K. Ulrich. The Five-Minute Oscillations on the Solar Surface. *Astrophysical Journal*, 162:993, December 1970.